Dispersing Carbon Nanotubes in Aqueous Solutions by a Starlike Block Copolymer

ARTICLE *in* THE JOURNAL OF PHYSICAL CHEMISTRY C · SEPTEMBER 2008

Impact Factor: 4.77 · DOI: 10.1021/jp8059344

Dispersing Carbon Nanotubes in Aqueous Solutions by a Starlike Block Copolymer

Xia Xin, Guiying Xu,* Taotao Zhao, Yanyan Zhu, Xiaofeng Shi, Houjian Gong, and Zhiqing Zhang

Key Laboratory of Colloid and Interface Chemistry, Shandong University, Ministry of Education, Jinan 250100, People's Republic of China

Received: July 05, 2008; Revised Manuscript Received: August 11, 2008

The ability of dispersing carbon nanotubes (CNTs) in aqueous solutions by a starlike amphiphilic block copolymer with PPO−PEO segments (AP432) was investigated in detail. For comparison, two commercially available linear amphiphilic block copolymers, Pluronics L64 and F127, were also selected. It was found that AP432 and F127 can get good CNT dispersions, while L64 was proved to be unable to disperse CNTs. AP432 with five branches could disperse CNTs efficiently at much lower concentrations compared with the linear F127, although it has a smaller molecular weight and shorter terminal EO groups. This indicated clearly that, once branched, copolymers would get a much better ability to disperse CNTs. Increasing concentration of AP432 or F127 would disperse more CNTs, but at high copolymer concentrations the aggregation of dispersed CNTs was observed, which may be related to the free micelles formed by AP432 or F127 around CNTs. Other influencing factors such as the mass ratio of CNTs to copolymers and sonication time and strength were also discussed. From the molecular dynamics simulation results, it can be found that copolymers with five branches can gain better steric repulsions between adjacent CNTs, which is consistent with the experimental results.

Introduction

Carbon nanotubes (CNTs) including single-walled carbon nanotubes (SWNTs) and multiwalled carbon nanotubes (MWNTs) have received great interest since their discovery[1,2] due to their unique properties and wide scope of possible applications.[3−9] However, a major barrier for CNT utilizations especially for SWNTs is their poor solubility and dispersability in both aqueous and organic media. They usually tend to form crystalline ropes due to strong intertube van der Waals attraction, leading to difficulties in their manipulation and incorporation into different matrixes. For successful utilization of their properties, uniform dispersions of CNTs in various media, especially in aqueous solutions, are required. Different approaches have been suggested to decrease the nanotube agglomeration such as ultrasonication and high shear mixing. In recent years, great efforts have been made to disperse CNTs into aqueous solutions by the noncovalent method[3,10−29] typically with the help of surfactants[10−15] or polymers[15−22] as well as natural macromolecules.[23−25] When mixed with CNTs, the hydrophobic parts of surfactants or polymers would interact with the sidewall of the CNTs, leaving their hydrophilic parts extending into water and impeding nanotube aggregation. Compared to chemical modification of CNTs, the noncovalent method has the advantage of no disruption of the structure and electronic properties of the native tubes.

For noncovalent methods, PEO−PPO−PEO block copolymers of the Pluronic series were frequently used for dispersing both SWNTs[15,17,18] and MWNTs.[30,31] Unlike ionic surfactants such as SDS[10−14] which prevent nanotube aggregation mainly by electrostatic repulsion, these copolymers impede nanotube aggregation mainly by the well-known steric repulsion. Hence, those with larger molecular weights and longer terminal EO groups would gain better ability to disperse SWNTs.[15] Up to now, however, all PEO−PPO−PEO copolymers used are the triblock copolymers with linear structures. The effect of branched block copolymers to disperse SWNTs remains unknown. Recently, a series of amphiphilic block copolymers with different molecular structures were synthesized in our laboratory, which were found to have many particular advantages in practical applications.[32,33] On the basis of a recent investigation of a starlike amphiphilic block copolymer with PPO−PEO segments (AP432),[34] we report in this paper the detailed investigation of its ability to disperse CNTs. To better clarify the effect of different molecular structures on dispersing CNTs, two commercially available linear PEO−PPO−PEO triblock copolymers of the Pluronic series, F127 ($EO_{97}PO_{69}EO_{97}$) and L64 ($EO_{13}PO_{30}EO_{13}$), were also selected. The results indicate that the starlike AP432 with five branches could disperse CNTs efficiently at much lower concentrations compared with the linear F127, although it has a smaller molecular weight and shorter terminal EO groups. Our experimental and simulation results may open the avenue of new applications for branched PPO−PEO block copolymers.

Experimental Section

Chemicals and Materials. CNTs were purchased from Shenzhen Nanotech Port Co., Ltd., which were prepared by the method of chemical vapor deposition (CVD) and contained ∼60% SWNTs and ∼35% MWNTs with a length of 2−15 μm. The remaining is mainly catalyst and amorphous carbon. The raw material was thoroughly characterized by TEM and Raman spectroscopy before use.

The amphiphilic block copolymer with starlike AP432 (Scheme 1) was synthesized by anionic polymerization in our laboratory following the procedures described previously.[34] The average molecular weight of AP432 was measured to be ∼7200 by gel permeation chromatography analysis, and the percentages

* To whom correspondence should be addressed. E-mail: xuguiying@sdu.edu.cn. Fax: +86-531-88564750.

10.1021/jp8059344 CCC: $40.75
Published on Web 09/25/2008

SCHEME 1: Molecular Details of Linear and Starlike Amphiphilic Block Copolymers[a]

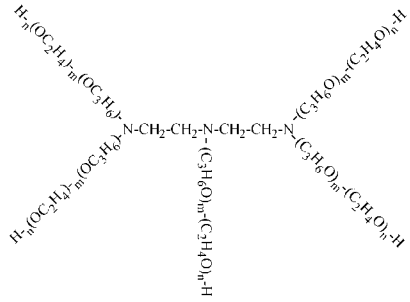

AP432 MW: 7200 EO wt% ≈ 37.4% m ≈ 15.5, n ≈ 12.2

F127: $(C_2H_4O)_{97}(C_3H_6O)_{69}(C_2H_4O)_{97}$

Linear MW: 12600 EO wt% ≈ 70%

L64 : $(C_2H_4O)_{13}(C_3H_6O)_{30}(C_2H_4O)_{13}$

Linear MW: 2900 EO wt% ≈ 40%

[a] The values of *m* and *n* for AP432 are the average values calculated according to the molecular weight and EO content.

of EO and PO were validated to be about 37.4% and 61.2% by ^{1}H NMR quantitative analysis, respectively. The linear triblock copolymers Pluronic F127 and L64 were obtained as a gift from BASF Corp. and used as received (the detailed information is shown in Scheme 1). Water used in the experiments was triply distilled by a quartz water purification system.

Instruments and Characterizations. UV−vis−NIR measurements were carried out on a computer-manipulated spectrometer (UV−vis 4100, Hitashi, Japan). The transmittance of the solution was measured at 500 nm with a Unico WFJ2000 spectrophotometer (Unico, Shanghai, People's Republic of China). Raman spectra were obtained from an NXR FT-Raman module (Nexus 670, Nicolet Co.) equipped with a Ge detector. The samples were excitated by a laser source with a wavelength of 1064 nm and a power of 0.103 W. TEM and HRTEM observations were carried out on a JEOL JEM-100 CXII (Japan) at an accelerating voltage of 80 kV and a JEOL JEM-2100 microscope (Japan) at an accelerating voltage of 200 kV, respectively. Samples were prepared by directly dipping a Formvar film-coated or ultrathin carbon-coated copper grid into the sample, which were then dried by using an NIR lamp before TEM or HRTEM observations were performed. An ultrasonicatior (KQ-250DB, Analytical Instrument Inc., Shanghai) with a frequency of 40 kHz and a maximum power of 250 W was used during sample preparation.

Sample Preparation. Stock aqueous solutions of 5 wt % AP432, F127, and L64 were prepared by dissolving the corresponding copolymer in water. The solutions were stored at room temperature (25 °C) for one week, during which gentle shaking was performed several times, ensuring dissolution of the copolymers. In a typical experiment, solid CNTs were weighed accurately into a vitreous bottle before copolymer stock solution and water were added. After sonication at 100 W and 40 kHz for 2 h, the samples were then stored at room temperature for sedimentation of large tube bundles before characterizations. In the experiments aiming at investigating the influence of sonication and sedimentation, the power of sonication was varied between 50 and 250 W and the time of sonication and sedimentation was also varied.

Molecular Simulation. Molecular simulations are performed by using the software Cerius^2 4.6. The COMPASS force field was selected. van der waals and Coulomb interactions were calculated using the atom-based cutoff method with a cutoff distance of 9.5 Å. All simulations were carried out in an NVT ensemble with a time step of 1 fs. The temperature was controlled using the Hoover−Nose thermostat at room temperature (298 K) with a relaxation time of 0.2 ps. The simulation time was 500 ps. According to the size of the SWNTs as well as the density of water, a periodic box was defined, into which a (12, 12) nanotube comprising 480 carbon atoms with a length of 40.8 Å was placed. Before simulation, the initial configuration was optimized by using the COMPASS force field and the "Smart Minimizer" method with "high-convergence" criteria.

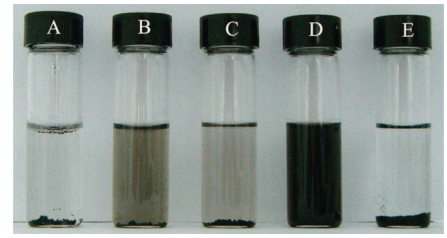

Figure 1. Dispersions of 1.0 mg of CNTs in 3 mL of aqueous solutions of 0.01 wt % F127 (A), 0.1 wt % F127 (B), 0.01 wt % AP432 (C), 0.1 wt % AP432 (D), and 5 wt % L64 (E). The samples were sonicated at 100 W and 40 kHz for 2 h and then stored at room temperature for at least two weeks before the photos were taken.

Results and Discussion

Dispersion Effect of Different Copolymers upon CNTs. The dispersion effects of CNTs in different solutions with AP432, F127, or L64 copolymers are presented in Figure 1. The amount of added CNTs was fixed at 1.0 mg, while the concentration of each copolymer was increased gradually to 5 wt %. For F127, it was found the CNTs could not be dispersed until their concentration reached 0.1 wt % (Figure 1A,B), while, for the starlike AP432, a slightly black dispersion was already observed after sonication even when its concentration was as low as 0.01 wt % (Figure 1C). When the concentration of AP432 reached 0.1 wt %, black dispersions which were stable for several months were obtained (Figure 1D). The color of this dispersion was much heavier than that obtained from F127 with the same concentration (Figure 1B), which could be easily seen by the naked eye. For another example, the transmittance of 1.0 mg of CNTs dispersed in 3 mL of 0.5 wt % AP432 at a wavelength of 500 nm was only 0.045, while that of 1.0 mg of CNTs dispersed in 3 mL of 0.5 wt % F127 treated at the same condition and recorded at the same wavelength was much higher, 0.262. This indicates clearly that AP432 could disperse more tubes into the bulk aqueous solutions than F127 by the same sample treatments. L64 was proved to be unable to disperse CNTs as its concentration was in the range of 0.1−5 wt %. This can be ascribed to its much lower molecular weight and shorter terminal EO groups, which could not create efficient steric repulsions between individual or small bundles of CNTs. A typical photo with a concentration of L64 of 5 wt % is also given for comparison (Figure 1E). It is evident that L64 has no ability to disperse CNTs, so we did not show its results in the following studies.

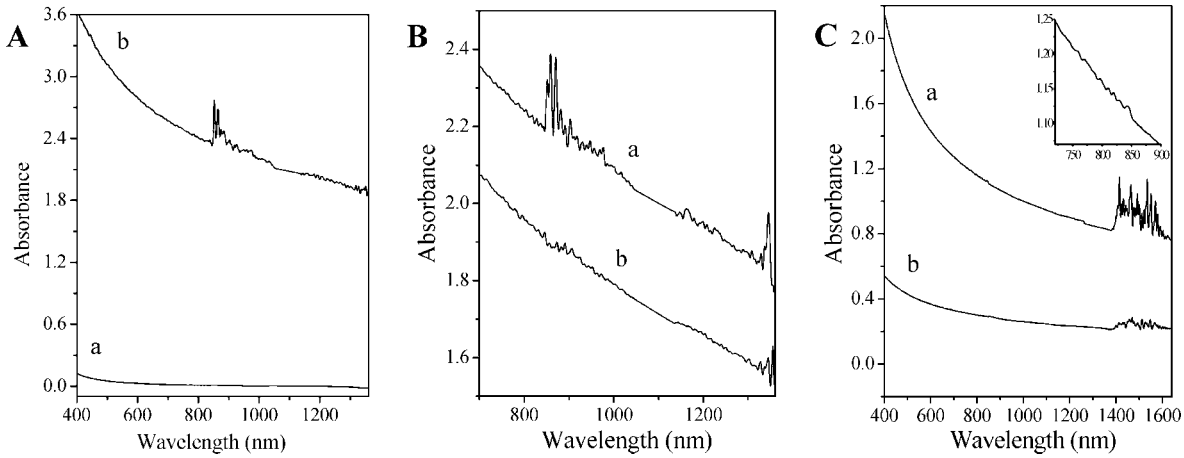

Figure 2. (A) UV−vis−NIR absorptions of 1 wt % AP432 aqueous solution (a) and a dispersion of 1.0 mg of CNTs in 3 mL of 1 wt % AP432 (b). The sample was sonicated at 100 W and 40 kHz for 15 min. (B) UV−vis−NIR measurements carried out 24 h (a) and 48 h (b) after sample preparation. The sample was the same as that in (A). (C) UV−vis−NIR absorptions of the dispersions for the two dispersions given in parts D (a) and B (b) of Figure 1. Measurements were carried out more than two weeks after sample preparation. The inset is the magnification of curve a.

Influence of the Sonication and Sedimention Time. The spectral features of CNT/AP432 dispersions as a function of the sonication and sedimentation time are summarized in Figure 2. For comparison, the spectral feature of the CNT/F127 dispersion is also shown. It can be seen from Figure 2 that aqueous solutions of pure AP432 display only negligible absorptions up to a concentration of 1 wt % (Figure 2A, curve a). After AP432 was mixed with 1.0 mg of CNTs and sonicated at 100 W and 40 kHz for 15 min, a macroscopic homogeneous black dispersion was obtained. After the dispersion was allowed to stand overnight, a small amount of precipitates could be found at the bottom of the dispersion. The slow precipitation process might be driven by the gradual formation of large bundles through encountered discrete CNTs.[35] The results of UV−vis−NIR measurement reveal the absorbance of the dispersion is higher than 2.0 across the 400−1360 nm region with several sharp absorption maxima located around 850 nm (Figure 2A, curve b). The absorptions beyond 1360 nm are too strong to be available. To observe the influences of the sonication time and sonication strength, two other samples were also prepared which were sonicated at 100 W and 40 kHz for 45 min and 250 W and 40 kHz for 15 min. Subsequent UV−vis−NIR measurements after the samples were allowed to stand overnight failed due to the very strong absorptions of the two samples in the entire wavelength range measured, clearly indicating that increasing time or strength of sonication is in favor of CNT dispersion in aqueous solutions.

Generally speaking, theory predicts that SWNTs have a variety of absorptions in the UV−vis−NIR region, which originates from energy levels with a significantly high density of states, called van Hove singularities,[36] formed during the rolling up of a 2D graphite sheet to a quasi-1D nanotube. The spectroscopic features of SWNTs depend only on their diameter and helicity.[37] Recent progress on dispersing SWNTs up to the single-tube level with the help of surfactants (typically SDS) has greatly accelerated identification of the spectroscopic features of SWNTs.[10−14] Typically, dispersed SWNTs have three sections of absorptions in the UV−vis−NIR region: the first van Hove transitions, E_{11}, of the direct band gap semiconducting tubes located at 800−1600 nm, slightly overlapping the 550−900 nm region of their E_{22} transitions and the lowest energy van Hove transitions of the metallic tubes located around 400−600 nm. In practice, however, one could only get the average spectroscopic characteristics of dispersed nanotubes because the SWNTs used are always a mixture which is polydisperse both in tube diameter and helicity. Thereforek, nanotubes from different sources would lead to subtle spectral differences. What's more, the spectral features of dispersions of SWNTs/surfactants or SWNTs/polymers also depend on the sonication and sedimentation times, which would affect the ultimate existing states of the tubes, i.e., bundles or individuals. Thus, results reported by different authors often differ from each other.[15]

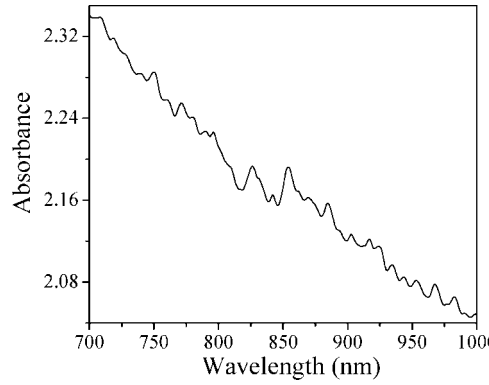

Figure 3. UV−vis−NIR absorption of a long time stored (more than one month) CNT/AP432 dispersion after resonication at 100 W and 40 kHz for ca. 10 min and then being left overnight. The sample was the same as that in Figure 2A.

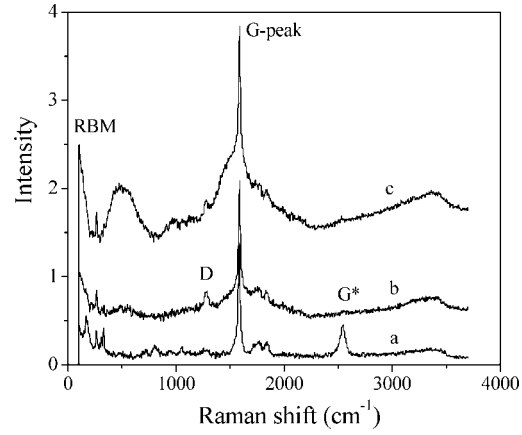

Figure 4. Raman spectra excited at 1064 nm of the raw CNTs (a) and 1.0 mg of CNTs dispersed in 3 mL of 0.05 wt% AP432 (b) and 1.0 mg of CNTs dispersed in 3 mL of 0.5 wt% AP432 (c).

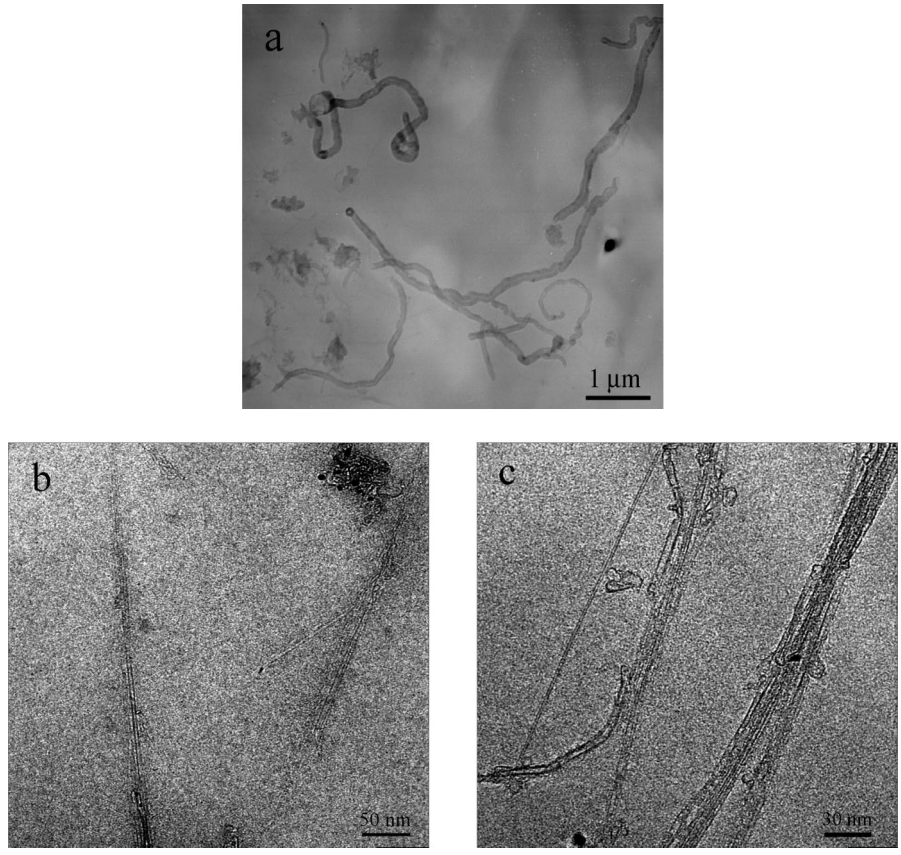

Figure 5. Typical TEM photograph of 1.0 mg of CNTs dispersed in 3 mL of 0.5 wt % AP432 aqueous solution (a) and HRTEM images of 1.0 mg of CNTs dispersed in 3 mL of 0.5 wt % AP432 aqueous solution (b) and 1.0 mg of CNTs dispersed in 3 mL of 0.5 wt % F127 aqueous solution (c).

Therefore, for our systems, if the dispersion was left standing for an extended period of time (48 h), sedimentation of CNTs continued as revealed by UV−vis−NIR measurements (Figure 2B) as well as visual inspection. However, it can be obviously found that the sedimentation speed of CNTs decreased. At this stage the absorbance intensity beyond 1360 nm was still too strong to be recorded. Finally after storage for about two weeks, the sedimentation of CNTs nearly ceased and the CNT/AP432 dispersions became extremely stable, plausibly due to the full protection of CNTs by the copolymers and hence negligible aggregation. UV−vis−NIR absorptions of the dispersions at this state for the two dispersions shown in Figure 1B,D are given in Figure 2C (the inset is the magnification of curve a). It can be seen that, with a further decrease of absorbance over the whole wavelength range, the absorption features of the metallic tubes and the E_{22} transition semiconducting tubes commonly located at ∼400−900 nm became not obvious and nearly negligible. At the same time, new rich absorptions were observed in the wavelength range of 1380−1600 nm, which corresponded to the E_{11} transitions of semiconducting tubes. From Figure 2C one can also see the absorption intensities of CNTs dispersed by AP432 (curve a) were much higher than those of CNTs dispersed by F127 (curve b) following the same sample treatment. This indicates AP432 could disperse more tubes than F127, which was also consistent with the macroscopic observations from Figure 1.

Furthermore, the CNTs precipitated at the bottom of the bottles could be well redispersed by sonication and re-formed a good dispersion, easier than the original raw CNT/AP432 mixtures. These precipitates should be a mixture of bundles of CNTs surrounded by AP432 molecules rather than pure CNTs.

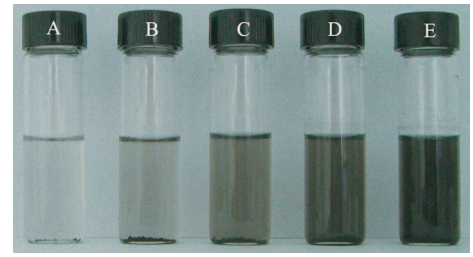

Figure 6. Dispersions of CNTs in 3 mL of 0.05 wt % AP432 aqueous solutions with increasing amount of added CNTs: 0.6 mg (A), 1.5 mg (B), 2.0 mg (C), 2.5 mg (D), 3.0 mg (E). The images were taken more than one month after preparation.

After redispersion, the absorptions of the metallic tubes and the E_{22} transition semiconducting tubes recovered. A typical UV−vis−NIR result of the redispersed sample recorded between 700 and 1000 nm is given in Figure 3.

Raman Spectra. Figure 4 summarizes the results of Raman spectra of the raw material and the CNT/AP432 dispersions with different compositions. Mainly three peaks of the radial breathing mode (RBM), which was known to be sensitive to the diameter but not the helicity of the tubes,[36] were observed for raw CNTs (curve a) with positions of about 167, 263, and 329 cm^{-1}. These correspond to a mean diameter of the tubes of 1.34, 0.85, and 0.69 nm, respectively, according to the following equation: $d = 223.75/\mathrm{RBM}$.[36] The tangential G-peak and G*-peak of the raw CNTs were located around 1587 and 2540 cm^{-1}, respectively. The D-peak, which was usually caused by defects in the CNTs,[38] was nearly negligible, indicating defects of the raw CNTs were rare.

After dispersion into the bulk aqueous solution of AP432, the position of the G-peak remained unchanged, as can be seen

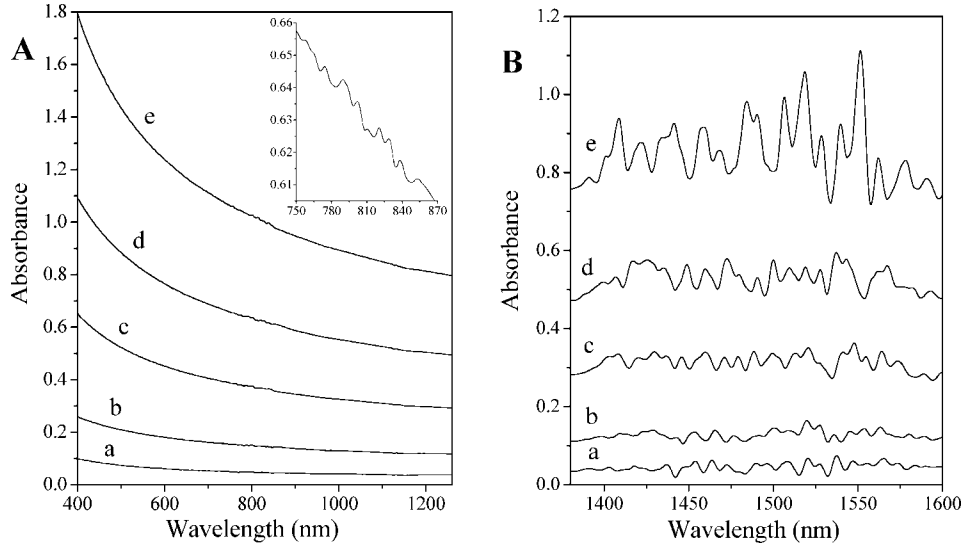

Figure 7. UV−vis−NIR absorptions in the (A) 400−1260 nm and (B) 1360−1600 nm regions for 0.05 wt % AP432/CNT dispersions. Curves a−e correspond to samples A−E in Figure 6. The inset of (A) is a magnified curve for curve d in the 750−870 nm region.

clearly from curves b and c in Figure 4, but the G*-peak diminished completely and the curves tend to protrude out of the baseline around 500 cm^{-1} and at higher wavenumbers, probably due to the resonance effect between dispersed CNTs and adsorbed AP432 molecules. For the RBM peaks, only the peak located around 263 cm^{-1} was still clear; the other two located around 167 cm^{-1} and 329 cm^{-1}, respectively, became not obvious. It seems that AP432 tends to selectively disperse CNTs with a certain value of diameter, which is 0.85 nm in our case. It is also seen from Figure 4 that the intensity of the D-peak of the dispersed CNTs is still small, indicating that the sonication conditions in our experiments do not cause obvious destructions on the nanotubes.

Morphology of the Dispersed Nanotubes. Upon storage at room temperature for one month, the CNTs dispersed by AP432 were still stable and showed a black color. TEM observations carried out at different magnifications revealed the existence of nanotubes with various diameters and lengths, and two typical images are shown in Figure 5a,b. The tubes usually tend to exist as individuals or very small bundles, which was in sharp contrast to the case of raw materials, and tend to aggregate into large ropes. For CNTs dispersed by copolymers, small bundles were frequently seen in the dispersion. This is because the hydrophobic parts of the copolymers with several tens of nanometers of full extended lengths tend to interact with the sidewalls of adjacent tubes rather than only one individual tube. Take the average distance of a C−C or C−O (in a zigzag mode) bond to be 0.1265 nm;[39] the full extended length of the PO groups of each branch of AP432 is calculated to be ∼7.8 nm, and it is already long enough to interact with more than one individual tube even for only one branch of the starlike AP432. According to this point, short chain ionic surfactants such as SDS are better candidates to get CNT dispersions of individual tubes than long-chain copolymers. However, in cases in which the amounts of dispersed CNTs in aqueous solutions are more concerned, copolymer-dispersed CNTs get great use because they could usually disperse more tubes than short-chain ionic surfactants such as SDS.

For CNTs dispersed by F127, a typical image of CNTs dispersed by F127 is also given in Figure 5c. The HRTEM observations showed that the bundles were usually much bigger than those found in AP432-dispersed samples, although individual tubes could also be seen. Probably several adjacent tubes were enlaced by F127 molecules, which have much longer PO groups (calculated to be ∼35 nm) compared with AP432. In other words, the starlike AP432 also has advantages to disperse CNTs as individuals or smaller bundles compared with the linear PEO−PPO−PEO block copolymer F127.

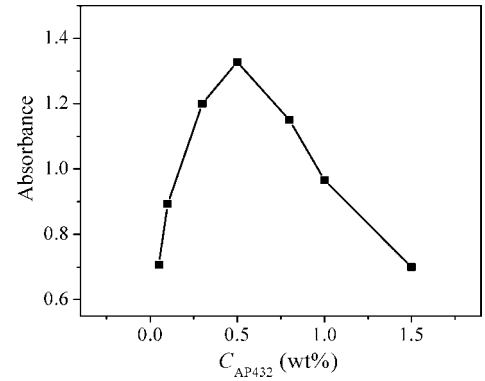

Figure 8. Absorbance intensity for the dispersion of 1.0 mg of CNTs dispersed in 3 mL of AP432 aqueous solutions as a function of the AP432 concentration (λ = 800 nm). The sample was sonicated at 100 W and 40 kHz for 15 min.

Influence of the CNT Amount. The effect of the amount of added CNTs on CNT/AP432 dispersions was investigated. A series of samples with 0.05 wt % AP432 and increasing amount of added CNTs are shown in Figure 6, and the UV−vis−NIR absorptions of their dispersions are given in Figure 7. It can be seen that with increasing amount of added CNTs, the color of the solutions becomes more and more black and their absorptions in both the 400−1260 nm (Figure 7A) and 1360−1600 nm (Figure 7B) regions increase correspondingly. This was because, as the amount of added CNTs was increased, more tubes were available to be dispersed into the bulk aqueous solutions. This experiment also indicated that AP432 has a high ability of dispersing CNTs, although its concentration was as low as 0.05 wt %.

Influence of the AP432 Concentration. To investigate the influence of micelle formation of AP432 on the stability of CNT/AP432 dispersions, UV−vis−NIR measurements were carried out on the dispersions of seven samples containing 1.0 mg of CNTs and 3 mL of aqueous solutions of AP432 with different concentrations after sonication and sedimentation. It was found

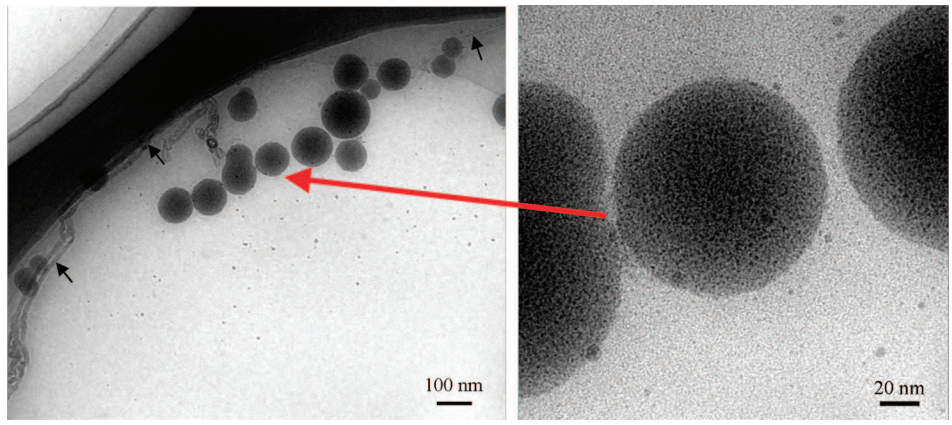

Figure 9. Micelles formed by AP432 in 1.0 mg of CNTs dispersed in 3 mL of 5 wt % AP432 aqueous solutions at different magnifications. Some CNTs can also be seen (black arrows).

the absorbance intensity did not increase continuously with increasing concentration. Instead, it passed through a maximum at an AP432 concentration of 0.5 wt % (exceeding the critical micellar concentration (cmc) of AP432) and then decreased (Figure 8). The influence of the AP432 concentration on CNT/AP432 dispersions was proved to be complicated. In a certain concentration range (≤0.5 wt %), increasing AP432 concentration would have a positive effect on the CNT dispersions, due to an increase of copolymers available for nanotube debundling,[40] but on the other hand, increasing the concentration of surfactants or copolymers would also cause a gradual increase of free surfactant or copolymer molecules in bulk aqueous solutions and finally lead to micelle formation when the concentration reaches the cmc. This induces an uncompensated force that results in a depletion attraction between adjacent CNTs, leading to the flocculation of dispersed CNTs. These effects induced by micelles have been observed and discussed in SDS-dispersed CNTs.[10,11] AP432 was known to easily form big and loose micelles in aqueous solutions as has been proved previously.[34] The cmc of AP432 is 120 mg·L^{-1}, and both the number and the size of the AP432 micelles increase with increasing of concentration of AP432.[34] This indicates that, at higher AP432 concentrations (>0.5 wt %), flocculation of dispersed CNTs occurred. Since AP432 could already form a large amount of micelles at a concentration of 5 wt % in CNT/AP432 mixtures, as revealed by HR-TEM observations (Figure 9), the flocculation of dispersed CNTs at higher concentrations of AP432 was very likely due to the depletion attraction induced by micelle formation.

However, the flocculation of dispersed CNTs at higher concentrations of AP432 could be partially or totally eliminated by increasing the mass ratio of initially added CNTs to AP432. At a higher amount of added CNTs and a higher concentration of AP432, for example, 3.0 mg of CNTs in 3 mL of 0.5 wt % AP432 aqueous solution, the dispersion became heavily black and ultimately opaque, preventing any characterizations even after sedimentation for more than a month. This was because more AP432 molecules were now required to debundle the CNTs, decreasing the concentration of AP432 in the bulk aqueous solution. Hence, the formation of micelles was greatly suppressed. For linear F127, which has a higher cmc value and forms smaller micelles compared with AP432, the micelle-induced flocculation of dispersed CNTs was less obviously seen in the investigated concentration range (0.01−1 wt %). At higher concentrations, however, similar phenomena have also been observed for CNT/F127 composites by others.[30] For example, Monteiro-Riviere et al. reported that F127 added at low

SCHEME 2: Schematic Representation of the Possible Mechanism for Nanotube Dispersion by AP432 and F127

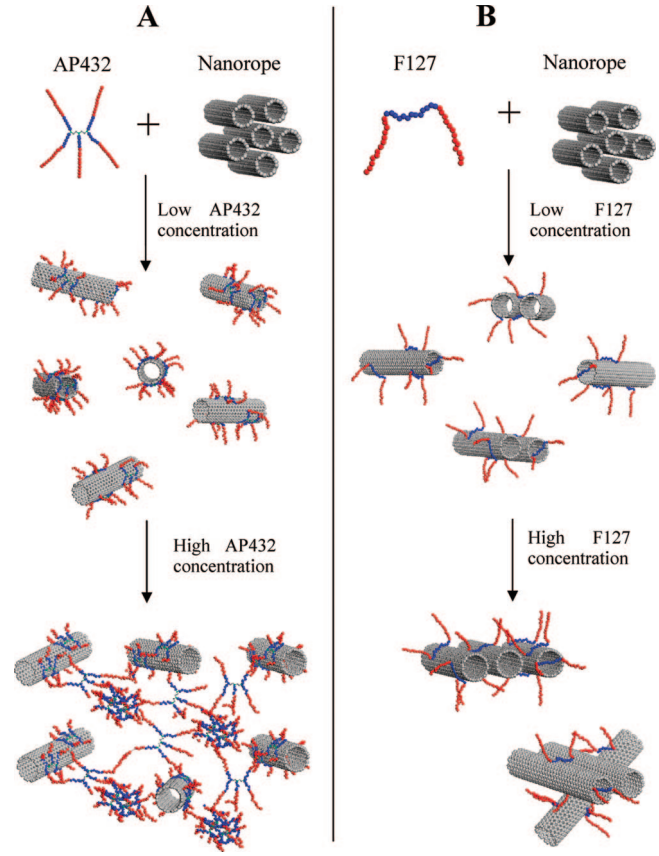

percentages had a positive effect on the tube debundling, but when the concentration of F127 reached 5 wt %, larger agglomerates were present that often resembled the nonsurfactant control samples.[30]

Mechanism of Dispersing CNTs by Copolymers. It has been well established that PEO−PPO−PEO triblock copolymers impede nanotube aggregation mainly by the well-known steric repulsion. When mixed with CNTs, the PO groups would interact with the sidewall of the CNTs (this kind of interaction was often called "wrap" or "decorate") while the EO groups would extend into water and hence create a so-called steric repulsion.[24] For this model, copolymers with larger molecular weights and longer terminal EO groups would gain a better ability to disperse CNTs, which has been proved to be true for

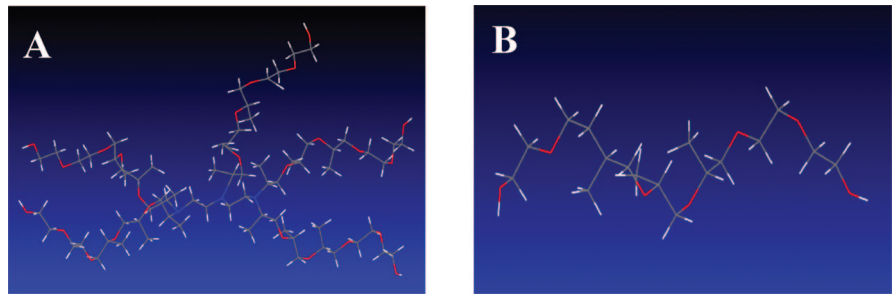

Figure 10. Configurations of the five-branched (A) and the linear (B) copolymer molecules.

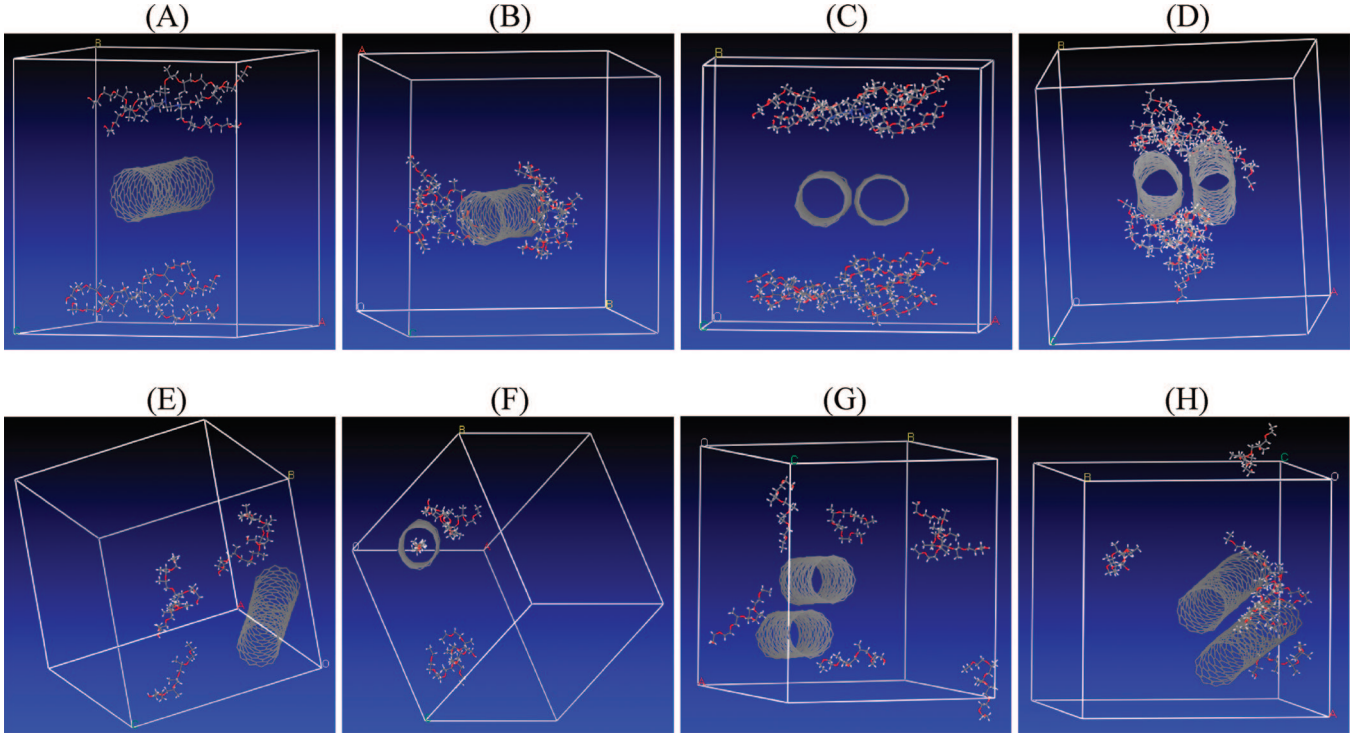

Figure 11. Snapshots of different block copolymer molecules adsorbed at the SWNT surface at 298 K: one SWNT and two five-branched copolymer molecules at the beginning (A) and end (B) of simulation, two SWNTs and four five-branched copolymer molecules at the beginning (C) and end (D) of simulation, one SWNT and five linear copolymer molecules at the beginning (E) and end (F) of simulation, two SWNTs and seven linear copolymer molecules at the beginning (G) and end of simulation (H).

many nonionic surfactants and PEO−PPO−PEO block copolymers of the Pluronic series with linear molecular structures.[15]

On the basis of HRTEM analysis and other observations mentioned above, the mechanism of dispersing CNTs by AP432 and F127 can be rationalized and is shown in Scheme 2; the starlike AP432 (Scheme 2A) has advantages in dispersing CNTs at much lower concentrations compared with the linear F127 (Scheme 2B), although it has a smaller molecular weight and shorter terminal EO groups. This abnormal phenomenon was undoubtedly ascribed to the difference between the molecular structures of AP432 and F127, which would cause two effects: (a) When mixed with CNTs in aqueous solutions, the number of hydrophilic EO groups extending into water per unit of CNTs is greater for AP432 compared with F127. This can be ascribed to the five branches of AP432, which could create a stronger steric repulsion. (b) With much shorter hydrophobic PPO segments located in five separated branches rather than one central part, each molecule of the starlike AP432 can interact with much smaller bundles or even individual tubes compared with F127. These two effects result in one point; that is, branched block copolymers have more advantages in dispersing CNTs at a much lower concentration and can get smaller tube bundles or even individuals.

Computer simulation is able to provide more microscopic level information than experiment.[41−43] Some researchers have studied the interaction between the polymer and CNTs by molecular dynamic (MD) simulations.[44,45] Although these studies cannot give bulk nanocomposite properties directly, they do provide us a clear and vivid view of the interface between the polymer and the CNTs. To validate and explain our experimental results, the interactions between different copolymers and SWNTs at low polymer concentrations are also investigated by MD simulations. The configurations of branched and linear copolymer molecules are presented in Figure 10, while the simulation results of interaction between different polymers and SWNTs are shown in Figure 11. From the results one can see that, for the system with only one tube (Figure 11A,E), the branched copolymers wrap tightly on the tube at the end of simulation (Figure 11B) while some of the linear copolymers can move into the tube and stay there due to their smaller volume (Figure 11F). For the system with two tubes (Figure 11C,G), the branched copolymers which have much bigger volumes than linear copolymers can adsorb between adjacent tubes, making the parallel tubes rotate (Figure 11D). A similar phenomenon has not been observed for linear copolymers (Figure 11H). Thus, it can be concluded that the

five-branched copolymer can gain better steric repulsions between adjacent SWNTs, which is consistent with our experimental results.

With increasing concentration of copolymers, micelles began to form which would then cause a depletion attraction and induce nanotube flocculation. Since branched copolymers have a much lower cmc value and could form much bigger micelles compared with linear ones as has been proved previously,[34] the micelle-induced nanotube flocculation could be more obviously seen for the starlike AP432 (Scheme 2A) than F127 (Scheme 2B). This problem, however, could be solved by raising the mass ratio of added CNTs to AP432. The starlike AP432 was proved to be a good candidate for nanotube isolation, and this conclusion can be well expected to extend to other branched block copolymers.

Conclusions

In summary, we have used a starlike block copolymer, AP432, to disperse CNTs in aqueous solutions, which shows advantages in dispersing ability against commercially available linear PEO−PPO−PEO block copolymers. The experimental and simulation results indicate that chemically branched block copolymers could get much better steric repulsions among the dispersed CNTs, which are necessary for the stabilization of CNT/copolymer dispersions. More tubes can be dispersed into the bulk aqueous solutions by carefully monitoring the experimental conditions including the amount of added CNTs and the concentration of AP432. At high concentration of AP432, free micelles began to form, which caused a subsequent flocculation of the dispersed tubes. Formation of stable dispersions can enable the testing of isolated tube properties and comparison to theoretical predictions. Our investigation also indicates that better copolymer/CNT dispersions can be obtained by simply changing the molecular structure of copolymers, i.e., from linear polymers to branched ones. This is in sharp contrast with previous investigations where attention has mainly been focused on improving the molecular weight of copolymers to get good copolymer/CNT dispersions and thus may open new avenues of CNT dispersion.

Acknowledgment. We gratefully acknowledge financial support from the Natural Science Foundation (Grant 20573067).

References and Notes

(1) Iijima, S. *Nature* **1991**, *354*, 56.
(2) Iijima, S.; Ichihashi, T. *Nature* **1993**, *363*, 603.
(3) Vaisman, L.; Wagner, H. D.; Marom, G. *Adv. Colloid Interface Sci.* **2006**, *128−130*, 37.
(4) Yang, Y. L.; Zhang, J.; Nan, X. L.; Liu, Z. F. *J. Phys. Chem. B* **2002**, *106* (16), 4139.
(5) Liu, C.; Fan, Y. Y.; Liu, M.; Cong, H. T.; Cheng, H. M.; Dresselhaus, M. S. *Science* **1999**, *286*, 1127.
(6) Sugie, H.; Tanemura, M.; Filip, V.; Iwata, K.; Takahashi, K.; Okuyama, F. *Appl. Phys. Lett.* **2001**, *78*, 2578.
(7) Zou, H. L.; Yang, Y. L.; Li, Q. W.; Zhang, J.; Liu, Z. F.; Guo, X. Y.; Du, Z. L. *Carbon* **2002**, *40* (12), 2282.
(8) Kong, J.; Franklin, N. R.; Zhou, C.; Chapline, M. G.; Peng, S.; Cho, K. *Science* **2000**, *287*, 622.
(9) Dai, H. J.; Hafner, J. H.; Rinzler, A. G.; Colbert, D. T.; Smalley, R. E. *Nature* **1996**, *384*, 147.
(10) Bonard, J. M.; Stora, T.; Salvetat, J. P.; Maier, F.; Stőchli, T.; Dischl, C.; Forró, L.; Heer, W.; Chatelain, A. *Adv. Mater.* **1997**, *9*, 827.
(11) Vigolo, B.; Pénicaud, A.; Coulon, C.; Sauder, C.; Pailler, R.; Kpirmet, C.; Bermoer, P. *Science* **2000**, *290*, 1331.
(12) O'Connell, M. J.; Bachilo, S. M.; Huffman, C. B.; Moore, V. C.; Strano, M. S.; Haroz, E. H.; Rialon, K. L.; Boul, P. J.; Noon, W. H.; Kittrell, C.; Ma, J.; Hauge, R. H.; Weisman, R. B.; Smalley, R. E. *Science* **2002**, *297*, 593.
(13) Bachilo, S. M.; Strano, M. S.; Kittrell, C.; Hauge, R. H.; Smalley, R. E.; Weisman, R. B. *Science* **2002**, *298*, 2361.
(14) Strano, M. S.; Dyke, C. A.; Usrey, M. L.; Barone, P. W.; Allen, M. J.; Shan, H.; Kittrell, C.; Hauge, R. H.; Tour, J. M.; Smalley, R. E. *Science* **2003**, *301*, 1519.
(15) Moore, V. C.; Strano, M. S.; Haroz, E. H.; Hauge, R. H.; Smalley, R. E. *Nano Lett.* **2003**, *3*, 1379.
(16) Nap, R.; Szleifer, I. *Langmuir* **2005**, *21*, 12072.
(17) Shvartzman-Cohen, R.; Nativ-Roth, E.; Baskaran, E.; Levi-Kalisman, Y.; Szleifer, I.; Yerushalmi-Rozen, R. *J. Am. Chem. Soc.* **2004**, *126*, 14850.
(18) Shvartzman-Cohen, R.; Levi-Kalisman, Y.; Nativ-Roth, E.; Yerushalmi-Rozen, R. *Langmuir* **2004**, *20*, 6085.
(19) Grunlan, J. C.; Liu, L.; Kim, Y. S. *Nano Lett.* **2006**, *6*, 911.
(20) Li, H.; Zhou, B.; Lin, Y.; Gu, L.; Wang, W.; Fernando, K. A. S.; Kumar, S.; Allard, L. F.; Sun, Y. P. *J. Am. Chem. Soc.* **2004**, *126*, 1014.
(21) Kang, Y.; Taton, T. A. *J. Am. Chem. Soc.* **2003**, *125*, 5650.
(22) Chen, J.; Liu, H.; Weimer, W. A.; Halls, M. D.; Waldeck, D. H.; Walker, G. C. *J. Am. Chem. Soc.* **2002**, *124*, 9034.
(23) Zheng, M.; Jagota, A.; Smeke, E. D.; Diner, B. A.; Mclean, R. S.; Lustig, S. R.; Richardson, R. E.; Tassi, N. G. *Nat. Mater.* **2003**, *2*, 338.
(24) Star, A.; Steuerman, D. W.; Heath, J. R.; Stoddart, J. F. *Angew. Chem., Int. Ed.* **2002**, *41*, 2508.
(25) Bandyopadhyaya, R.; Nativ-Roth, E.; Regev, O.; Yerushalmi-Rozen, R. *Nano Lett.* **2002**, *2*, 25.
(26) Zhu, J.; Yudasaka, M.; Zhang, M.; Iijima, S. *J. Phys. Chem. B* **2004**, *108*, 11317.
(27) Chen, R. J.; Zhang, Y.; Wang, D.; Dai, H. *J. Am. Chem. Soc.* **2001**, *123*, 3838.
(28) Nakashima, N.; Tomonari, Y.; Murakami, H. *Chem. Lett.* **2002**, *31*, 638.
(29) Nakashima, N.; Tanaka, Y.; Tomonari, Y.; Murakami, H.; Kataura, H.; Sakaue, T.; Yoshikawa, K. *J. Phys. Chem. B* **2005**, *109*, 13076.
(30) Monteiro-Riviere, N. A.; Inman, A. O.; Wang, Y. Y.; Nemanich, R. J. *Nanomedicine* **2005**, *1*, 293.
(31) Vaisman, L.; Marom, G.; Wagner, H. D. *Adv. Funct. Mater.* **2006**, *16*, 357.
(32) Zhang, Z. Q.; Xu, G. Y.; Wang, F. *J. Colloid Interface Sci.* **2005**, *282*, 1.
(33) Wang, F.; Xu, G. Y.; Zhang, Z. Q.; Xin, X. *Eur. J. Inorg. Chem.* **2006**, *1*, 109.
(34) Xin, X.; Xu, G. Y.; Zhang, Z. Q.; Chen, Y. J.; Wang, F. *Eur. Polym. J.* **2007**, *43*, 3106.
(35) Collins, P. G.; Arnold, M. S.; Avouris, P. *Science* **2001**, *292*, 706.
(36) Saito, R.; Dresselhaus, G.; Dresselhaus, M. S. *Phys. Rev. B* **2000**, *61*, 2981.
(37) Bandow1, S.; Asaka, S.; Saito, Y.; Rao, A. M.; Grigorian, L.; Richter, E.; Eklund, P. C. *Phys. Rev. Lett.* **1998**, *80*, 3779.
(38) Chen, X.; Lee, G. S.; Zettle, A.; Betozzi, C. R. *Angew. Chem., Int. Ed.* **2004**, *43*, 6111.
(39) Tanford, C. *J. Phys. Chem.* **1972**, *72*, 3020.
(40) Zhang, Q.; Lippits, D. R.; Rastogi, S. *Macromolecules* **2006**, *39* (2), 658.
(41) Frankland, S. J. V.; Caglar, A.; Brenner, D. W.; Griebel, M. *J. Phys. Chem. B* **2002**, *106*, 3046–3048.
(42) Liao, K.; Li, S. *Appl. Phys. Lett.* **2001**, *79*, 4225–4227.
(43) Gou, J.; Minaie, B.; Wang, B.; Liang, Z. Y.; Zhang, C. *Comput. Mater. Sci.* **2004**, *31*, 225–236.
(44) Yang, M. J.; Koutsos, V.; Zaiser, M. *J. Phys. Chem. B* **2005**, *109*, 10009–10014.
(45) Zheng, Q. B.; Xue, Q. Z.; Yan, K. Y.; Hao, L. Z.; Li, Q.; Gao, X. L. *J. Phys. Chem. C* **2007**, *111*, 4628–4635.

JP8059344